Turkish Journal of Electrical Engineering & Computer Sciences

http://journals.tubitak.gov.tr/elektrik/

Research Article

Turk J Elec Eng & Comp Sci
(2017) 25: 4636 – 4646

doi:10.3906/elk-1703-131

Optimal reactive power flow in BDFMs for converter cost reduction and efficiency improvement

Behzad JANDAGHI[1], **Hamed GORGINPOUR**[2], **Mohammad Naser HASHEMNIA**[3,*], **Hashem ORAEE**[1]

[1]Department of Electrical Engineering, Sharif University of Technology, Tehran, Iran
[2]Engineering Department, Persian Gulf University, Bushehr, Iran
[3]Department of Engineering, Mashhad Branch, Islamic Azad University, Mashhad, Iran

Received: 11.03.2017 • **Accepted/Published Online:** 15.09.2017 • **Final Version:** 03.12.2017

Abstract: A brushless doubly fed machine is equipped with two decoupled windings on its stator, known as the power winding and the control winding. The power winding reactive power can be controlled by voltage amplitude fed by the machine-side converter to the control winding, affecting both the converter size and machine efficiency. This paper investigates different proposed scenarios for optimal reactive power flow targeted to minimize the converter cost and maximize the machine efficiency. Previously, the grid-side converter has not been used for reactive power compensation. However, in the present paper it is shown how the grid-side converter can be effectively used to reduce the converter cost by controlling the flow of reactive power. The optimal power winding reactive powers for minimizing the converter cost and for maximizing the output power are not the same. Then the priority of minimizing converter cost over maximizing machine output power has been justified.

Key words: Brushless doubly fed machine, equivalent circuit, maximum output power, minimum converter cost, optimal reactive power flow

1. Introduction

The application of a brushless doubly fed machine (BDFM) as an adjustable speed drive and generator is studied in [1,2]. BDFMs have some advantages over doubly fed induction machines, including improved reliability and lower maintenance costs due to the absence of the brush gear, a lower gearbox ratio as a result of lower rotational speed, and better low-voltage ride-through capability [3].

On the other hand, some drawbacks, including lower efficiency arising from poor machine design, motivate further investigations on optimal design and control of BDFMs.

As illustrated in Figure 1, the BDFM has two windings on its stator, known as the power winding (PW) and the control winding (CW). The PW is connected to the grid directly and the CW is connected by a partially rated bidirectional converter, which allows the machine to operate in a desirable speed range. To avoid direct electromagnetic coupling between the two windings, their pole-pair numbers should be different [4]. The rotor is typically of nested loop design, the number of nests being equal to summation of PW and CW pole-pair numbers. This enables indirect cross-coupling between the two stator windings.

The machine has three modes of operation: simple induction mode (when the CW is open circuited),

*Correspondence: hashemnia@mshdiau.ac.ir

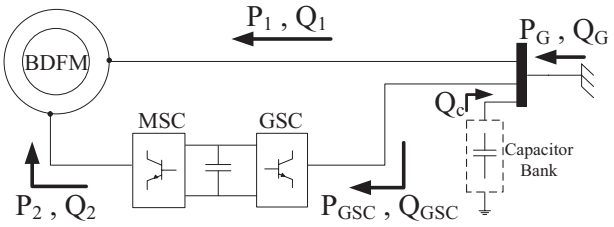

Figure 1. BDFM configuration and the power flow conventions.

cascade induction mode (when the CW is short circuited), and synchronous mode (when both PW and CW are supplied). The last one is the most desirable mode for BDFM operation [4]. In synchronous mode of operation, both PW and CW are supplied, and the machine speed varies with the PW and CW frequencies independent of the value of the torque up to the stability margin, as in:

$$\omega_r = \frac{\omega_1 + \omega_2}{p_1 + p_2}, \tag{1}$$

where ω_1 and ω_2 are electrical angular frequencies of PW and CW, respectively, p_1 and p_2 are their corresponding pole-pair numbers, and ω_r is the rotor mechanical speed.

When the CW is supplied by a DC voltage the machine operates at its natural speed, as follows:

$$\omega_n = \frac{\omega_1}{p_1 + p_2} \tag{2}$$

The performance of a BDFM is investigated in [5]. Back-to-back converters, consisting of the machine-side converter (MSC) and the grid-side converter (GSC), are widely used in variable frequency systems. The machine torque and the PW reactive power can be controlled separately through appropriate CW excitation by MSC [6–9]. The GSC is mainly used to keep the DC link voltage constant, regardless of the power flow direction, by regulating the CW active power, and to control the grid power factor generally by supplying reactive power to the grid [10].

The partially rated power converter for doubly fed machines makes the overall system economical, and so determination and minimization of the converter rating would be important to commercialize the BDFM. Furthermore, efficiency is also important to deliver the maximum active power to the grid as a generator. In [11], the converter rating of a 7-kW prototype BDFM is minimized through the CW voltage. In addition, it is shown that the optimal CW excitations for minimum inverter rating and maximum power output for a given machine speed are not necessarily the same. However, the optimal CW excitation as a compromise between the two schemes is not investigated. The optimal stator windings design is also investigated in [12] to maximize the output power and minimize the converter rating [13]. In [14], utilization of the GSC and capacitor bank to reduce the converter rating is investigated through a PW flux-oriented control scheme. However, the optimal rating for the two converters and the optimal capacitor bank is not introduced. In [15–20], optimal reactive power allocation between MSC and GSC was studied for DFIGs to minimize the converter rating. Recently, the largest manufactured BDFM, with a rating of 250 kW, was experimentally tested and reported in [21], which is used in this paper as the case study. This paper shows the higher efficiency of the machine in comparison to the 7 kW prototype BDFM reported in [11].

In this paper, first the BDFM equivalent circuit is introduced, and the active and reactive power flows are presented. Then a criterion for the converter cost is proposed, and the PW reactive power is used to

minimize the total converter cost at specific operating conditions. Afterwards, the optimal PW reactive power to maximize the output power or machine efficiency is obtained. In the following, the priority of controlling the PW reactive power to minimize the converter cost over maximizing the machine output is illustrated, and finally the optimal PW reactive power is derived to maximize the efficiency with minimized converter rating. This study is based on a nonideal per-phase equivalent circuit referred to PW, which is introduced in the subsequent section.

2. Equivalent circuit model

The equivalent circuit, whose parameters can be measured experimentally, is shown in Figure 2 [22].

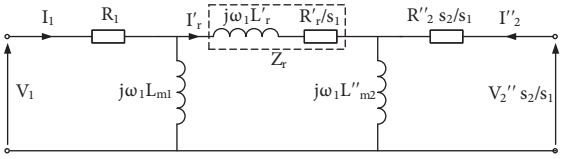

Figure 2. Per-phase BDFM equivalent circuit referred to the PW.

In this figure, s_1 and s_2 are the rotor slips with respect to PW and CW, respectively, defined by:

$$s_1 = \frac{\omega_1 - p_1\omega_r}{\omega_1}, \quad s_2 = \frac{\omega_2 - p_2\omega_r}{\omega_2} \tag{3}$$

The parameters of the studied prototype BDFM are reported in [21].

Using the equivalent circuit, the CW quantities referred to PW can be calculated as a function of PW quantities through Eq. (4).

$$\begin{pmatrix} \frac{s_2}{s_1}V_2'' \\ I_2'' \end{pmatrix} = \begin{pmatrix} A & B \\ C & D \end{pmatrix} \begin{pmatrix} V_1 \\ I_1 \end{pmatrix}, \tag{4}$$

where A, B, C, and D are defined as follows:

$$A = \frac{\frac{R_r' R_2'' s_2}{s_1^2} - \omega_1^2 L_{m2}'' \left(L_{m1} + L_r'\right) + j\omega_1 \left[\frac{R_r' L_{m2}''}{s_1} + R_2'' \frac{s_2}{s_1}\left(L_{m1} + L_r' + L_{m2}''\right)\right]}{-\omega_1^2 L_{m1} L_{m2}''} \tag{5}$$

$$B = \frac{\frac{R_1 R_r' R_2'' s_2}{s_1^2} - \omega_1^2 L_{m2}''\left(L_{m1} + R_1 L_{m1} + L_r'\right) - \frac{\omega_1^2 L_{m1} R_2'' s_2}{s_1}}{\omega_1^2 L_{m1} L_{m2}''} + \frac{j\omega_1 \left[\frac{R_1 R_r' L_{m2}''}{s_1} - \omega_1^2 L_{m1} L_r' L_{m2}'' + R_2'' \frac{s_2}{s_1}\left(\frac{L_{m1} R_r'}{s_1} + R_1\left(L_{m1} + L_r' + L_{m2}''\right)\right)\right]}{\omega_1^2 L_{m1} L_{m2}''} \tag{6}$$

$$C = \frac{\frac{R_r'}{s_1} + j\left(L_{m1} + L_r' + L_{m2}''\right)}{-\omega_1^2 L_{m1} L_{m2}''} \tag{7}$$

$$D = \frac{R_1 R_r'}{s_1} - \omega_1^2 L_{m1}\left(L_r' + L_{m2}''\right) + j\omega_1 \left[R_1\left(L_{m1} + L_r' + L_{m2}''\right) + L_{m1}\frac{R_r'}{s_1}\right], \tag{8}$$

where R_1, R_r', and R_2'' are the PW, rotor, and CW resistances, respectively; L_{m1} and L_{m2}'' are PW- and CW-magnetizing inductances, respectively; and L_r' is the rotor leakage inductance.

2.1. Active and reactive power flow

The simplified equivalent circuit of BDFM, which only contains rotor leakage reactance ($jw_1L'_r$), is shown in Figure 3. Active and reactive power flow can be analyzed using the power diagram in Figure 4.

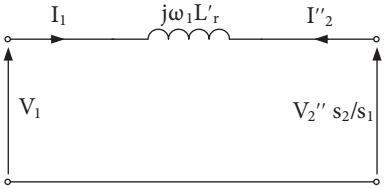

Figure 3. Simplified per-phase BDFM equivalent circuit referred to the PW.

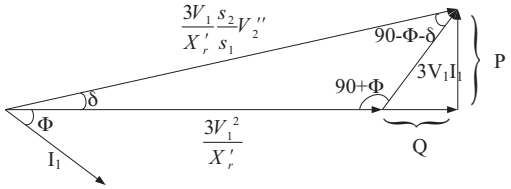

Figure 4. BDFM power diagram.

The active and reactive power flow in a simplified BDFM can be calculated as follows:

$$P = \frac{3\,V_1}{X'_r}\,\frac{s_2}{s_1}\,V''_2 \sin\delta \tag{9}$$

$$Q = \frac{3\,V_1}{X'_r}\,\left(\frac{s_2}{s_1}\,V''_2 \cos\delta - V_1\right), \tag{10}$$

where V_1 is PW voltage, V''_2 is CW voltage referred to PW side and δ is its corresponding angle, and X'_r is the rotor leakage reactance evaluated at PW frequency.

It can be concluded that reactive power flow can be controlled by CW voltage at a certain speed (certain s_2/s_1) and a certain torque (certain load angle δ). Eqs. (9) and (10) are presented for the simplified machine. However, in a real BDFM, the power flow is rather different. In a real BDFM, when $s_2/s_1\,V''_2\cos\delta$ is equal to V_1, the machine reactive power is supplied by both PW and CW being used mainly in the PW- and CW-magnetizing inductances. Increasing the CW voltage (over-exciting) increases the contribution of CW in supplying machine reactive power and decreases the PW reactive power to zero. Further increment in CW voltage results in exporting reactive power from PW to the grid. In a similar way, the reactive power flow reverses when the CW voltage decreases [23]. The per-phase BDFM equivalent circuit of Figure 2 can be used to analyze the machine under different operating conditions with an acceptable accuracy. All required machine variables, including PW and CW voltages, currents, active and reactive powers, and power factors, as well as speed, efficiency, converter ratings, etc. are involved in the equivalent circuit model. The parameters can be changed and monitored to determine machine behavior under different operating conditions.

Figure 5 shows the variation in the PW power factor via CW voltage in 320 rpm and 3760 Nm generating torque. The PW phase voltage is 690 V.

2.2. Optimal reactive power flow to minimize the converter cost

This section aims to determine the optimal MSC and GSC ratings for the prototype BDFM as reported in [21]. The characteristics of a switch that affect the converter cost include its rated current in conduction mode, which is dependent on the operating condition, and the reversed bias voltage, which is imposed by the DC link voltage.

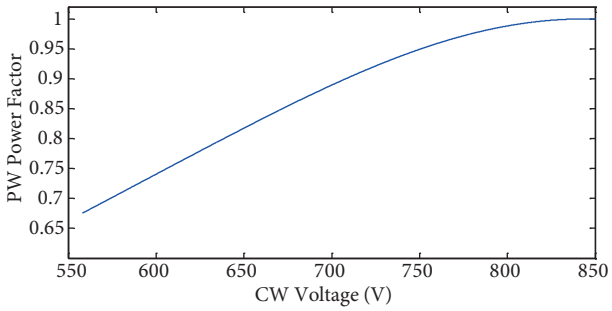

Figure 5. PW power factor against CW voltage.

For appropriate operation of the PWM converter, the DC link voltage (V_{DC}) should be greater than the peak value of the line to line supplied voltage [24], i.e.:

$$V_{DC} \geq \sqrt{2} V_{LL}, \tag{11}$$

where, for bidirectional power flow,

$$V_{LL} = \max\{V_G,\ V_{CW}\}, \tag{12}$$

where V_{LL}, V_G, and V_{CW} are the effective values of line-to-line voltage, GSC voltage, and CW voltage, respectively. In order to minimize the converter cost, the reference V_{DC} should be set at the minimum value of (11). It can be shown that for specified lagging PW power factors, the desired speed range, and the CW-to-PW turns ratio, the CW voltage is generally lower than PW or grid voltage, and so the grid voltage is the key determinant factor for the DC link voltage value. It can be concluded that converter cost minimization necessitates minimization of the converter current. Therefore, the objective function is defined as the summation of MSC current (I_{MSC}) and GSC current (I_{GSC}), as follows:

$$J = I_{MSC} + I_{GSC}, \tag{13}$$

where

$$I_{MSC} = I_2'' \tag{14}$$

$$I_{GSC} = \frac{\sqrt{P_2^2 + (Q_1 - Q_c \pm |P_1 + P_2| \tan(\cos^{-1} GPF))^2}}{\sqrt{3} \times V_1}, \tag{15}$$

where I_2'' is CW current referred to PW side, P_1 and P_2 are respectively output powers of PW and CW, V_1 is PW voltage, Q_1 is PW reactive power, Q_c is the capacitor bank reactive power, "+" stands for leading, and "-" stands for lagging grid power factor.

The PW voltage is 690 V_{rms} and the constraints of the problem are presented in Table 1.

Table 1. Constraints of the optimization problem.

Speed variation range	320–680 rpm	PW rated current	178 A	
Torque	1000–3760 Nm generating mode	CW rated current	73 A	
Grid power factor	0.9–1 lag	CW rated voltage	620 V	

Table 2. Comparison of the three different approaches.

	MSC current (A)	GSC current (A)	Total current (A)	Machine efficiency (%)	Output power (kW)
Approach 1	112	65	177	91–96	105–255
Approach 2	84	64	148	92–96	110–260

The speed range of the doubly fed machines affects the required converter size. Conventionally, the rotor speed is considered to have ±36% deviation from the natural speed [19]. For the prototype machine with 2/4 pole-pair windings supplied by a 50 Hz grid frequency, the speed range would be in the range of 320–680 rpm.

To find the worst case in machine operation, based on which the converter rating should be determined, the torque should be considered at its maximum value. Furthermore, it will be shown that the grid power factor should be set to unity in order to obtain the required converter rating.

In the optimization, the PW- and CW-rated currents as well as the CW voltage limits should not be violated. The maximum value of the CW voltage is dictated by the DC link voltage. Since the minimum DC link voltage has been considered, the maximum CW voltage that the converter can produce is the grid voltage.

2.3. Conventional operation

Conventionally, the GSC is used only to fix the DC link voltage. Thus, the minimum rating of the GSC can be determined as $|P_2|$. As a result, the grid reactive power, related to the operating point, passes through the PW. Figures 6 and 7 show the MSC and GSC currents versus machine speed according to this approach for three different grid power factors, i.e. 0.9 lagging, unity, and 0.9 leading. The maximum value of the graphs can be considered as the MSC- and GSC-rated currents.

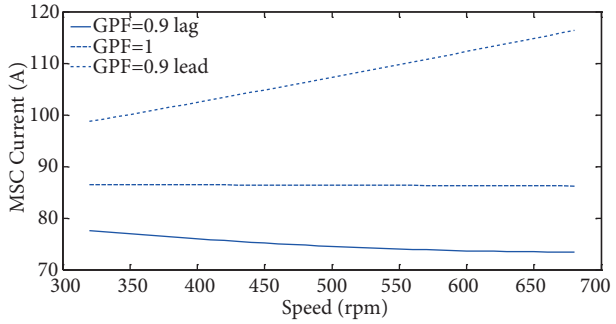

Figure 6. Variation in the MSC current via machine speed with different power factors.

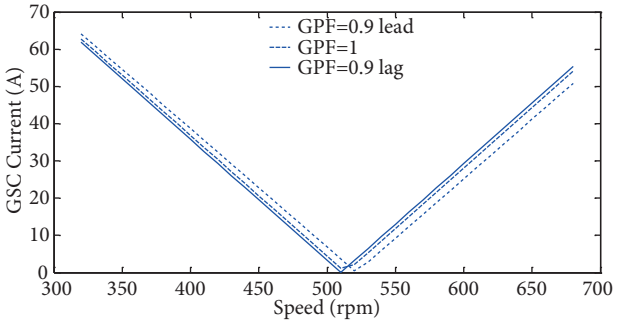

Figure 7. Variation in the GSC current via machine speed with different power factors.

It can be concluded that increasing the grid power factor increases the converter current. Hence, to satisfy the constraint of the optimization problem, the grid power factor should be kept at unity.

2.4. Optimal reactive power flow

As active and reactive power flows were described, absorbing reactive power through the PW decreases the MSC current, since the CW needs to pass less reactive power. Reduction of the converter size by absorbing reactive power through the PW has some restrictions, including changing the grid power factor, which is a constraint. The other constraint is PW-rated current. For the prototype BDFM, the rated torque, i.e. 3670 Nm, can be applied to the machine in a PW reactive power range of –100 to +200 kVArs. Both converters can

be used for optimal reactive power flow to minimize the total converter cost. Absorbing reactive power by the PW decreases the CW reactive power. On the other hand, the grid power factor constraint should be satisfied. Thus, one approach can be proposed by absorbing reactive power by the PW and satisfying the grid power factor using GSC ability in generating reactive power. It should be mentioned that this approach decreases the MSC current and increases GSC current in comparison with the currents achieved in the last approach. As a result, an optimal value for the PW reactive power can be found to minimize the summation of MSC and GSC currents. Figure 8 shows the effect of PW reactive power and grid power factor on total converter current, using the GSC to compensate the PW reactive power to keep the grid power factor at a certain value. In the simulation, the grid power factor is varied in the range of 0.9 lagging to unity. Worst-case turbine mechanical torque is considered to be 3760 Nm. It is demonstrated in Figure 8 that increasing the grid power factor from 0.9 lagging to unity increases the required converter current. Hence, unity grid power factor should be considered.

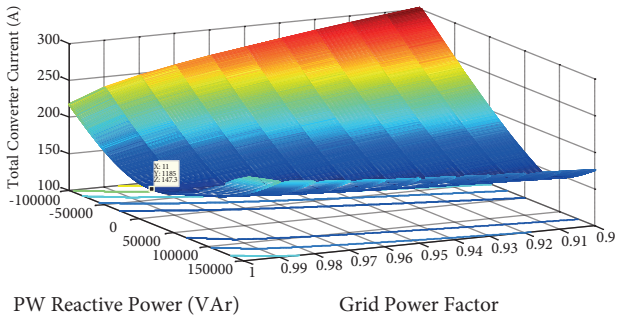

Figure 8. Total converter current via PW reactive power and grid power factor.

It can be concluded that, under the desired operating conditions, absorbing 18 kVArs by the PW will minimize the total converter current in this case study.

Table 2 shows the comparison of the MSC and GSC currents, output power, and efficiency in the speed range for the two following approaches:

Table 3. Output power in 320 rpm with different torques.

Output power (kW)	Approach 1	Approach 2	Approach 3
3760 Nm	113	107	107
3000 Nm	94	87	94
2000 Nm	64	57	64
1000 Nm	62	56	62

- Approach 1: Conventional approach: The GSC power factor is kept at unity.

- Approach 2: Optimal reactive power flow: The GSC reactive power flow ability is used to generate the optimal PW reactive power in order to keep the grid power factor at unity.

Approach 2 achieves a reduction in converter rating using the ability of the GSC in generating reactive power to fix the grid power factor. The extent of the reduction is 16.3% in comparison with the conventional approach. In addition, it is shown that an improvement in machine efficiency, especially at lower speeds, can be obtained using this approach.

2.5. Optimal reactive power flow to maximize output power or efficiency

Machine efficiency can be calculated using Eq. (16):

$$\text{Efficiency} = \frac{P_1 + P_2}{T\omega_r} \tag{16}$$

Considering BDFM as a generator, maximizing efficiency corresponds to maximizing the active output power in a certain torque and rotational speed. Figure 9 shows the machine output power variation versus the PW reactive power. In the simulation, the machine rotating speed is 680 rpm and the torque is 3760 Nm.

For each rotational speed and torque, an optimal reactive power for the PW can be found to maximize efficiency. Figure 10 shows the optimal reactive power in different torques to maximize machine efficiency at 680 rpm.

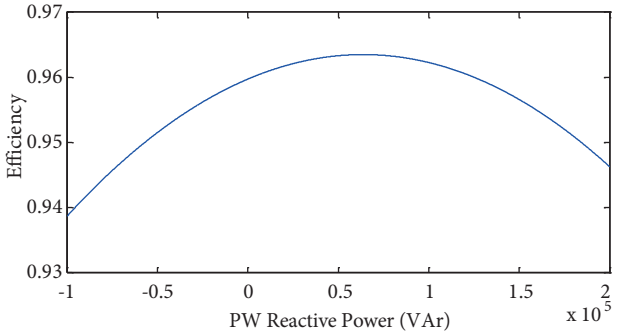

Figure 9. Machine efficiency variations via PW reactive power.

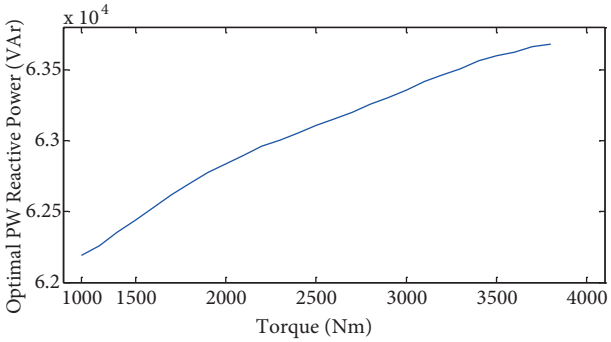

Figure 10. Optimal PW reactive power to maximize machine efficiency in different torques.

2.6. Overall optimal reactive power flow

The optimal reactive power values for minimization of the converter current and maximization of the machine efficiency are not the same. As shown in the previous sections, the PW needs to pass more reactive power in order to maximize the power output than to minimize the converter cost. Thus, to achieve the optimal PW reactive power, the importance of the objective functions should be investigated. It is worth noting that the converter-rated currents are determined based on the worst case of the operation range, i.e. the maximum torque and lower limit of the speed (Figures 6 and 7). The converters' capacity is not fully used at lower torques and certain speeds. With the determined rating for the MSC and GSC converters, the unused capacity can be used to improve machine efficiency. Therefore, an optimization problem can be defined to find the optimal reactive power to reach the maximum output power with the MSC and GSC rated currents as a constraint obtained in section 4. The optimization flowchart is presented in Figure 11.

In the flow chart, first the machine equivalent circuit parameters, the input torque, speed range, and the PW reactive power range are used to find the optimized ratings for MSC and GSC. Then the PW reactive power is changed in an optimization loop in order to find the maximum output power, while the MSC and GSC ratings are not violated. In other words, the optimized GSC and MSC converter ratings act as the problem constraint for the PW optimal reactive power flow.

The results of the optimization problem are obtained for the machine speed of 320 rpm with different input torques in Table 3, and for 3760 Nm torque with different speeds in Table 4. In the tables, the output active power is determined with three approaches:

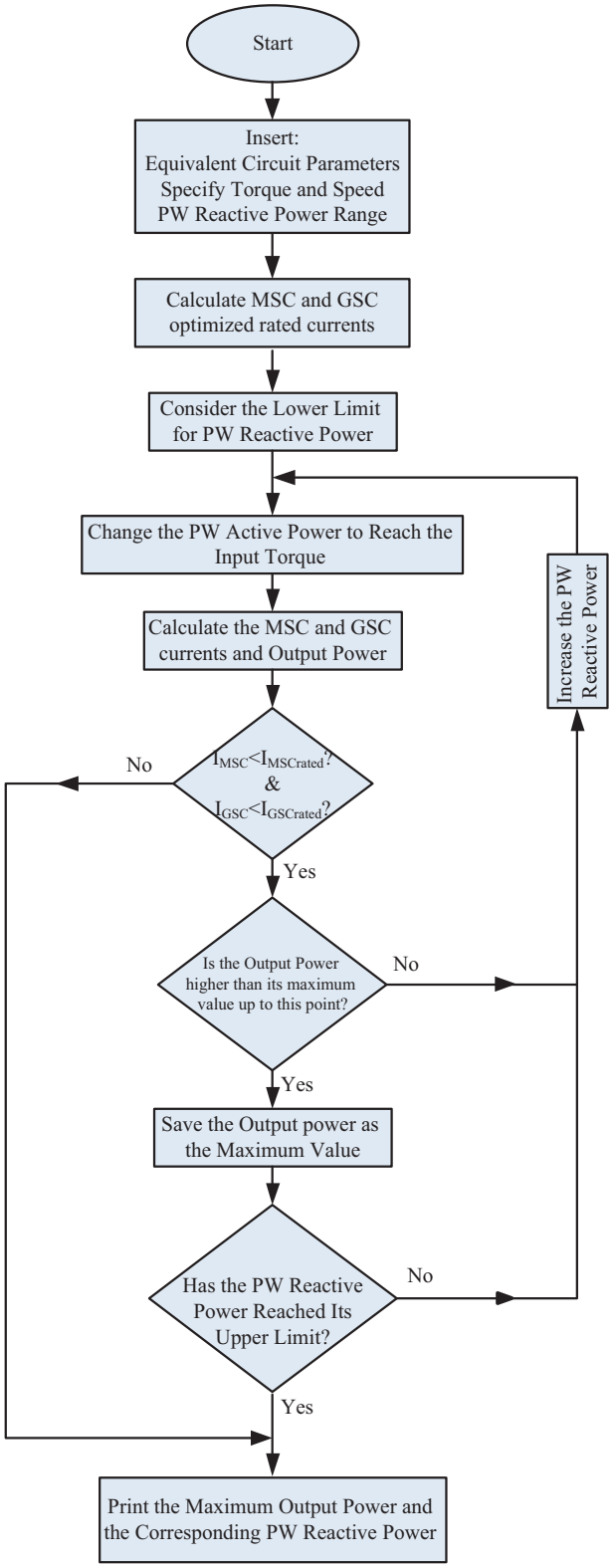

Figure 11. Optimization flowchart.

Table 4. Output power in 3760 Nm with different speeds.

Output power (kW)	Approach 1	Approach 2	Approach 3
320 rpm	113	107	107
450 rpm	163	157	163
550 rpm	202	195	202
680 rpm	252	245	252

- Approach 1: Maximum output power that can be achieved by optimal reactive power flow without the converter rating constraints.
- Approach 2: The output power achieved using converter cost minimization strategy.
- Approach 3: Optimal reactive power to achieve the maximum output power with minimized MSC- and GSC-rated current constraints.

It can be concluded that the output power can reach its maximum value in the majority of machine operating ranges. In practice, the converter size (nominal voltage and current) and the variable capacitor bank can be determined in the design stage as soon as the capacity of the generator is determined. The minimum converter size required for the control winding and the capacitor can be installed using the proposed scheme upon unit installation. To maximize machine efficiency, a look-up table is generated in the design stage based on the proposed method to be used as the reference of the control system for optimal reactive power flow to minimize the machine loss. In other words, the converter rating and capacitor bank are determined based on the full load (independent of the operating point) and the optimal reactive power flow is controlled through the look-up table (dependent on the statistical load). Although measurement errors offered by CTs and PTs for current and voltage measurements can slightly affect the optimal reactive power flow, the installed converter size and capacitor bank would not be affected since they are designed based on the full load current.

3. Conclusion

It is shown how reactive power flow can be used to minimize converter cost and maximize machine efficiency. Furthermore, it is illustrated that the two optimization problems have a conflict with each other, i.e. optimal reactive power flow to minimize the converter cost limits the output active power, and optimal reactive power flow to maximize the output power requires higher converter cost, in turn. It is shown that minimizing the converter rating should be considered as the first priority, since maximum output power can be obtained in the majority of the machine operating ranges.

References

[1] Wallace AK, Spée R, Lauw HK. The potential of brushless doubly-fed machines for adjustable speed drives. In: IEEE 1990 Pulp and Paper Industry Technical Conference; 18 June 1990; New York, NY, USA: IEEE. pp. 45-50.

[2] Brune C, Spee R, Wallace A. Experimental evaluation of a variable-speed, doubly-fed wind-power generation system. IEEE T Ind Appl 1994; 30: 648-655.

[3] Long T, Shao S, Abdi E, Malliband P, Mathekga ME, McMahon RA, Tavner PJ. Symmetrical low voltage ride-through of a 250 kW brushless DFIG. In: IET 2012 International Conference on Power Electronics, Machines and Drives; 27–29 March 2012; Bristol, UK: IET. pp. 1-6.

[4] Roberts PC. A study of brushless doubly-fed (induction) machines. PhD, University of Cambridge, Cambridge, UK, 2004.

[5] Tohidi S, Zolghadri, M, Oraee H, Tavner P, Abdi E, Logan T. Performance of the brushless doubly-fed machine under normal and fault conditions. IET Electr Power App 2012; 6: 621-627.

[6] Poza J, Oyarbide E, Sarasola I, Rodriguez M. Vector control design and experimental evaluation for the brushless doubly fed machine. IET Electr Power App 2009; 3: 247-256.

[7] Shao S, Abdi E, Barati F, McMahon R. Stator-flux-oriented vector control for brushless doubly fed induction generator. IEEE T Ind Electron 2009; 56: 4220-4228.

[8] Barati F, McMahon R, Shao S, Abdi E, Oraee H. Generalized vector control for brushless doubly fed machines with nested-loop rotor. IEEE T Ind Electron 2013; 60: 2477-2485.

[9] Shao S, Abdi E, McMahon R. Low-cost variable speed drive based on a brushless doubly-fed motor and a fractional unidirectional converter. IEEE T Ind Electron 2012; 59: 317-325.

[10] Carlson R, Voltolini H. Grid synchronization of brushless doubly fed asynchronous generators in wind power systems. In: IEEE 2008 International Conference on Industrial Electronics; October 2008; Montevideo, Uruguay: IEEE. pp. 2173-2177.

[11] Wang X, Roberts PC, McMahon RA. Studies of inverter ratings of BDFM adjustable speed drive or generator systems. In: IEEE 2005 International Conference on Power Electronics and Drives Systems; 16 January 2006; Kuala Lumpur, Malaysia: IEEE. pp. 337-342.

[12] Wang X, Roberts PC, McMahon RA. Optimisation of BDFM stator design using an equivalent circuit model and a search method. In: 3rd IET 2006 Power Electronics, Machines and Drives Conference; 4 April 2006; Dublin, Ireland: IET. pp. 606-610.

[13] Abdi E, Oraee A, Abdi S, McMahon RA. Design of the brushless DFIG for optimal inverter rating. In: IET 2014 International Conference on Power Electronics, Machines and Drives; 8–10 April 2014; Manchester, UK: IET. pp. 4-4.

[14] Carlson R, Voltolini H, Runcos F, Kuo-Peng P, Batistela NJ. Performance analysis with power factor compensation of a 75 kw brushless doubly fed induction generator prototype. In: IEEE 2007 International Electric Machines & Drives Conference; 3 May 2007; Antalya, Turkey: IEEE. pp. 1502-1507.

[15] Abbey C, Joos G. Optimal reactive power allocation in a wind powered doubly-fed induction generator. In: IEEE 2004 Power Engineering Society General Meeting; 10 June 2004; Denver, CO, USA: IEEE. pp. 1491-1495.

[16] Abbey C, Joós G. A systematic approach to design and operation of a doubly fed induction generator. Electr Pow Syst Res 2008; 78: 399-408.

[17] Aguglia D, Viarouge P, Wamkeue R, Cros J. Analytical determination of steady-state converter control laws for wind turbines equipped with doubly fed induction generators. IET Renew Power Gen 2008; 2: 16-25.

[18] Troncoso PE, Battaiotto PE, Mantz RJ. Active and reactive power control capability in wind generation based on BDFIG machine. In: Innovative Smart Grid Technologies Latin America; 5–7 October 2015; Montevideo, Uruguay: IEEE PES. pp. 546-551.

[19] Oraee A, Abdi E, McMahon RA. Converter rating optimisation for a brushless doubly fed induction generator. IET Renew Power Gen 2014; 9: 360-367.

[20] Oraee A, Abdi E, Abdi S, McMahon RA. A study of converter rating for Brushless DFIG wind turbines. In: IET 2007 Renewable Power Generation Conference; 9 September 2013; Beijing, China: IET. pp. 1-4.

[21] McMahon RA, Abdi E, Malliband PD, Shao S, Mathekga ME, Tavner PJ. Design and testing of a 250 kW medium-speed brushless DFIG. In: IET 2012 Power Electronics, Machines and Drives Conference; 27 March 2012; Bristol, UK: IET. pp. 1-6.

[22] Roberts PC, McMahon RA, Tavner PJ, Maciejowski JM, Flack TJ. Equivalent circuit for the brushless doubly fed machine (BDFM) including parameter estimation and experimental verification. IEE P-Elect Pow Appl 2005; 152: 933-942.

[23] McMahon RA, Roberts PC, Wang X, Tavner PJ. Performance of BDFM as generator and motor. IEE P-Elect Pow Appl 2006; 153: 289-299.

[24] Junchuan J, Weiguo L. Control characteristic of three-phase voltage-source PWM rectifier. Electric Power Automation Equipment 2010; 30: 63-65.